

# Sparse Inverse Chirp-Z Transform of S-Parameter Measurements for Time Domain Analysis of Transmission Line

Guilherme H. Weber, Hector L. Moura, Guilherme Dutra, Uilian J. Dreyer, Rafael J. Daciuk, Jean C. C. da Silva, Cicero Martelli, Daniel R. Pipa, Marco J. da Silva.

**Abstract**—Time-domain analysis of S-Parameters can be performed by converting data collected in the frequency to time domain. Although the use of the Chirp Z Transform approach, a more general Fourier transform tool, flexibilizes data acquisition, the conversion (or inversion) becomes difficult. Most existing methods approximate the Inverse Chirp Z transform by a minimum norm solution, which does not have strong physical support. In this paper, we propose a Sparse Inverse Chirp Z transforms specially crafted for sparse time-domain signals representing spikes generated at impedance discontinuities. The method is verified by comparing time-domain results of S-Parameters extracted of a cascaded transmission line set to the ones given by ADS Keysight® software, showing good agreement in reflection and transmission behavior of the line.

**Keywords**— ICZT, Sparse Analysis, S-Parameters, Time-domain Analysis.

## I. INTRODUCTION

Reflectometry methods are well established for locating faults on electric cables and transmission lines, and have been extensively used in past. The main approach is to apply a high-frequency stimulus to the line and monitor the reflected signals that are generated at impedance mismatches. Among the methods, one can highlight Time Domain Reflectometry (TDR), Frequency Domain Reflectometry (FDR) [1], [2], time gating methods [3], and identification of moderate reflections of cascaded circuits by transmissions and reflections measurements [4]. Most of them have their application restricted by certain assumptions such as small amplitudes for the reflections [4], [5] or prior knowledge about the line under test [6]. Recently, a method has been proposed for locating and separating closely spaced reflections with high magnitude using a sample maximum likelihood estimator, however at the expense of an increase in complexity of the model [7].

Time-domain methods may not be applied to monitor weak impedance mismatches or at high noisy and/or high attenuation systems due to limits of signal detection [8]. In addition, time-domain reflectometry methods require ideal open and short terminations, which are difficult to achieve over a broadband frequency range. Open circuit terminations cause stray capacitance due to electric field fringing at high frequencies, while short circuit terminations introduce additional inductance [9].

The analysis of the transmission line using the concept of travelling waves has presented itself as a more attractive alternative. Specifically, the scattering parameters depend solely on incident, scattered and reflected waves over the network, and

not on the terminations. Additionally, the electric cable can be examined with a vector network analyzer (VNA) which provides high signal-to-noise ratio (SNR) and high frequency resolution over a wide bandwidth since measurements are made at one frequency at a time. Once determined, the scattering parameters in time domain provide an impedance profile of the line under test, useful for evaluating impedance variations and faults along the line.

In order to convert frequency-domain information to the more usual time-domain traces, one possible method is based on Inverse Chirp Z Transform, which is already in use by a number of commercial instruments. Nevertheless, since the very nature of discontinuities is sparse, we aim in this work to investigate a Sparse Inverse Chirp Z Transform as an inversion method for conversion of frequency to time domain data in fault location and impedance profile of transmission lines.

## II. THE CHIRP Z TRANSFORM

Lawrence Rabiner has proposed the Chirp Z Transform in 1969 [10], which consists of an algorithm that evaluates the Z transform of a sequence of  $N$  samples at  $M$  points in the  $Z$  plane, standing either right on circular or spiral contours beginning at any arbitrary point. The Chirp Z Transform can be interpreted as a generalization of the DFT (Discrete Fourier Transform), which is restricted to the unit circle in the  $z$  plane.

For a given  $N$ -sample sequence  $\{x(n)\}$  with  $0 \leq n \leq N-1$ , the Chirp Z Transform is defined as (1)

$$X(k) = \sum_{n=0}^{N-1} x[n] (AW^{-k})^{-n}, \quad (1)$$

where  $X(k)$  is the resulting sequence, sampled in  $M$  points and  $0 \leq k \leq M-1$ .  $A$  and  $W$  are arbitrary complex numbers defined by (2) and (3)

$$A = A_0 e^{j2\pi\theta_0} \quad (2)$$

$$W = W_0 e^{-j2\pi\phi_0}, \quad (3)$$

with  $A_0$  as the starting radius,  $\theta_0$  the starting angle, and  $\phi_0$  the angle step size [11]. The rate at which the contour spirals in or out from a circle of radius  $A_0$  is set by the constant  $W_0$ . If less than 1, the contour spirals out. If greater than 1, the contour spirals in [10].

The term  $AW^{-k}$  configures the contour at which the  $z$  transform will be defined in the  $z$  plane. Fig. 1 shows a plot of

Guilherme Heim Weber, Hector Lise de Moura, Guilherme Dutra, Uilian José Dreyer, Rafael José Daciuk, Jean Carlos Cardozo da Silva, Cicero Martelli, Daniel Rodrigues Pipa, Marco José da Silva, Federal University of Technology – PR (UTFPR), Curitiba-PR, Brazil, E-mails: [gweber@alunos.utfpr.edu.br](mailto:gweber@alunos.utfpr.edu.br), [hector@alunos.utfpr.edu.br](mailto:hector@alunos.utfpr.edu.br), [gdutra@alunos.utfpr.edu.br](mailto:gdutra@alunos.utfpr.edu.br), [uiliand@alunos.utfpr.edu.br](mailto:uiliand@alunos.utfpr.edu.br), [daciuk@utfpr.edu.br](mailto:daciuk@utfpr.edu.br), [jeancs@utfpr.edu.br](mailto:jeancs@utfpr.edu.br), [cmartelli@utfpr.edu.br](mailto:cmartelli@utfpr.edu.br), [danielpipa@utfpr.edu.br](mailto:danielpipa@utfpr.edu.br), [m.dasilva@ieee.org](mailto:m.dasilva@ieee.org).

the contour in the  $z$  plane. For the sake of completeness, if  $A = 1$ ,  $M = N$  and  $W = e^{j2\pi/N}$ , one obtains the DFT.

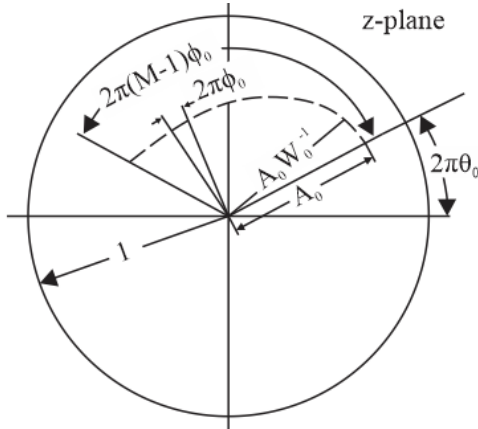


Fig. 1. Spiral contour in the  $z$  plane for the Chirp Z Transform.

The main advantages offered by the Chirp Z Transform are: there is no need for the input sample to be the same as the size of the output sample; neither  $N$  nor  $M$  need be composite numbers, both can be primes; the angular spacing along the contour is arbitrary, which gives also arbitrary frequency resolution; the starting point of analysis in the  $Z$  plane is also arbitrary, which is useful for narrow-band analysis.

If data are collected in the frequency domain with a Vector Network Analyzer (VNA), an Inverse Chirp Z Transform (ICZT) is required to convert the signals to the time-domain, where one is able to perform better analysis. Mersereau [12] presents an algorithm to calculate the inverse chirp z transform using the relation given by  $ICZT(X(k)) = A^n CZT(1, W^{-1}, C_k X(k), N)$ , where  $C_k$  is a calculated coefficients array. However, it is mentioned that the number of problems to which the proposed algorithm might be applied can be extremely sensitive to quantization errors. Frickey [11] proposes that the Inverse Chirp Z Transform can be accomplished by  $ICZT(X(k)) = [CZT(X(k)^*)]^*$ , though no performance guarantee is given for the CZT that operates outside the unit circle in the  $z$  plane. Yagüe et al. [13] approaches the problem by a direct method though (4)

$$x(t_1 + n\delta t) = \frac{1}{M} \sum_{k=0}^{M-1} X(k) e^{j2\pi(f_1 + k\delta f)(t_1 + n\delta t)} \quad (4)$$

$$n = 0, 1, \dots, N-1$$

where  $x(t_1 + n\delta t)$  denotes the time domain data,  $f_1$  and  $t_1$  the start frequency and time respectively,  $\delta f$  and  $\delta t$  the step frequency and time respectively.

The arbitrariness of CZT in choosing the number of samples, whether in frequency or in time, is not just an advantage but it also brings matters in the inverse problem. The difference between the number of input and output samples can render the inversion unstable due to ill-posedness of the problem. This issue will be further examined in Section IV.

### III. TIME DOMAIN ANALYSIS BASED ON S PARAMETERS

Commonly referred to S-parameters, scattering parameters are widely used for characterizing  $n$ -port networks. Rather than voltages and currents, the logical variables related to the network behavior are traveling waves. They relate the waves scattered or reflected from the network to those waves incident upon the network [14]. From the scattering parameters it is possible to extract the characteristic impedance, propagation constant and

distributed parameters (resistance, inductance, conductance and capacitance) of the line [9].

For a given 2-port network, the S-matrix (5) represents the relationship between the normalized incident voltage waves (independent variables  $a_1$  and  $a_2$ ) and the normalized reflected voltage waves (dependent variables  $b_1$  and  $b_2$ ):

$$\begin{bmatrix} b_1 \\ b_2 \end{bmatrix} = \begin{bmatrix} S_{11} & S_{12} \\ S_{21} & S_{22} \end{bmatrix} \begin{bmatrix} a_1 \\ a_2 \end{bmatrix} \quad (5)$$

S-parameters are extracted by terminating one or the other port with the normalizing impedance  $Z_0$  (normally  $50 \Omega$  for commercial network analyzers), instead of short or open circuit terminations like is made in methods for characterizing based on reflectometry principle. The topology for measuring S-parameters is shown in Fig. 2.

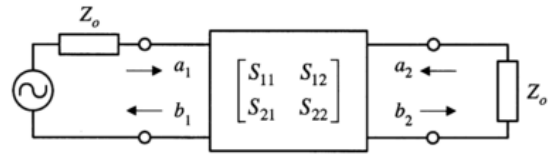


Fig. 2 - Scattering parameters measurement topology for 2-port network [9].

The parameter  $S_{11}$  is the input reflection coefficient with matched output,  $S_{21}$  the forward transmission coefficient with matched output,  $S_{22}$  the output reflection coefficient with matched input, and  $S_{12}$  the reverse transmission coefficient with matched input [14]. In other words,  $S_{11}$  and  $S_{22}$  are related with how matched is the network (referenced to  $Z_0$ ), whereas  $S_{21}$  and  $S_{12}$  give a meaning for how the network will attenuate or amplify an input signal.

The S-parameters are given in frequency domain and a conversion method is required to perform time domain reflectometry analysis. Network analyzers usually provide proprietary methods for the conversion over which the user has little or no control.

### IV. THE SPARSE INVERSE CHIRP Z TRANSFORM

The Chirp Z Transform can be cast in a matrix format (6)

$$X = Cx \quad (6)$$

where  $C$  is a  $M \times N$  matrix (called CZT matrix) that implements (1).

If  $M=N$ ,  $C$  implements a DFT and the inverse is given by  $C^*$  (conjugate transpose) since  $C$  becomes unitary. The general CZT matrix, however, can be interpreted as a modified DFT matrix, where some rows were modified, added or discarded. Either way, the inverse is no longer  $C^*$ .

Most ICZT approaches approximate the inverse by  $C^*$ . This may provide poor results, especially when rows were discarded. The result is the minimum norm solution (7)

$$x = C^* (CC^*)^{-1} X \quad (7)$$

which does not have strong physical support.

Instead, we propose a sparse reconstruction, where one wants to find a signal, sparse in time, representing the reflections along the line. The reconstruction method can be formulated by an L2-L1 minimization problem, where one has an L2 data-fidelity term and an L1 sparse promoting term (8)

$$x = \arg \min \|Cx - X\|^2 + \lambda \|x\|_1, \quad (8)$$

where  $\lambda$  the regularization parameter, and  $x$  the estimated solution.

The Fast Iterative Shrinkage-Thresholding Algorithm (FISTA) is an efficient first-order method for minimizing a composite convex cost function (L2) with a convex non-smooth term (L1) [15]. In this work, the choice for FISTA was made due to its simple implementation and fast convergence. By solving (8) with FISTA, the obtained solution  $x$  will be a sparse signal representing the reflection coefficients on the transmission line.

## V. EXPERIMENTAL

To evaluate the proposed method for frequency to time domain data conversion, a circuit composed by series connected transmission lines was simulated using the software ADS Keysight® Technologies (under Student License). In the simulation there are five lines connected, named as TLD1-TLD5. Their characteristic impedance and time delay are 50  $\Omega$  10.101 ns, 75  $\Omega$  10.101 ns, 50  $\Omega$  5.0505 ns, 75  $\Omega$  10.101 ns, and 50  $\Omega$  5.0505 ns respectively. Both ends of the line are terminated in 50  $\Omega$ . The simulated circuit is shown in Fig. 3.

The alias free range [16] defines that the maximum time for sampling is given by (9):

$$t_{\max} = \frac{1}{2\delta f}. \quad (9)$$

Considering twice the total time delay of the line under test (round trip), 80.808 ns, the step frequency for this analysis shall be nearly about to 6.1875 MHz. Using the low pass mode set [8], the first frequency for the analysis shall be equal to the step frequency. The frequency span gives the resolution that will be reached [17] (10):

$$Resolution = \frac{0.5 * delay}{\Delta F}. \quad (10)$$

Since the whole line delay is about 80.808 ns, with resolution within 5 % of the delay line the frequency span will be about 9.9 GHz. With 1601 sampling points, the parameters set is defined: 6.1875 MHz for frequency step, 1601 points, start frequency also in 6.1875 MHz and stop frequency in 9.9061875 GHz.

The scattering parameters were extracted and compiled into a s2p touchstone file. From this file data in frequency domain were extracted and processed by an algorithm in MATLAB® that performs the conversion to time domain using the proposed method. White Gaussian noise was introduced to the data in frequency domain before the conversion in the algorithm, turning the evaluation more real with a SNR of 5 dB. The converted data is then compared to the data in time domain given by the TDR Front Panel Option available in the ADS software.

The experimental setup was built using real transmission lines with equal simulation parameters described, from the frequency sweep parameters to the characteristics of the lines. The scattering parameters were acquired by a VNA E5071C

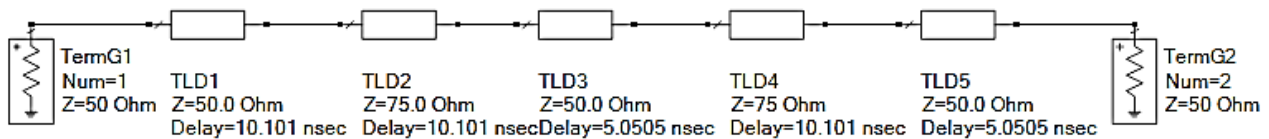


Fig. 3 - Transmission line simulated composed by five sections: TLD1 (50 Ohms 10.101 ns), TLD2 (75 Ohms 10.101 ns), TLD3 (50 Ohms 5.0505 ns), TLD4 (75 Ohms 10.101 ns), and TLD5 (50 Ohms 5.0505 ns).

Keysight® and also processed by the algorithm developed. In this case white Gaussian noise was not added, since it is intrinsically presented in the measured data. Results are compared to data in time domain obtained by transient analysis (available in the ADS software) of the scattering parameters acquired from the measurements. Fig. 4 shows a flow chart for the operation of the algorithm.

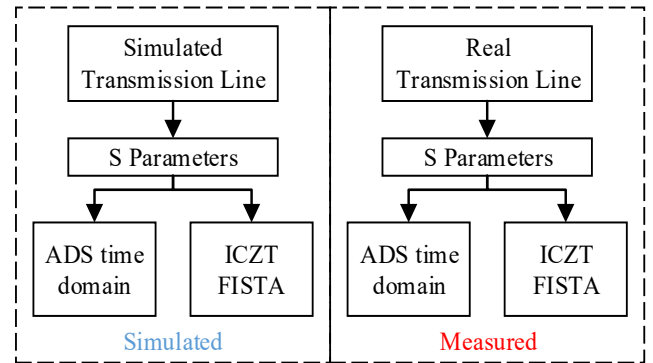


Fig. 4 - Algorithm flowchart.

## VI. RESULTS AND DISCUSSION

Results in time domain for  $S_{11}$  and  $S_{21}$  parameter of the simulated line are shown in Fig. 5 and Fig. 6 respectively.

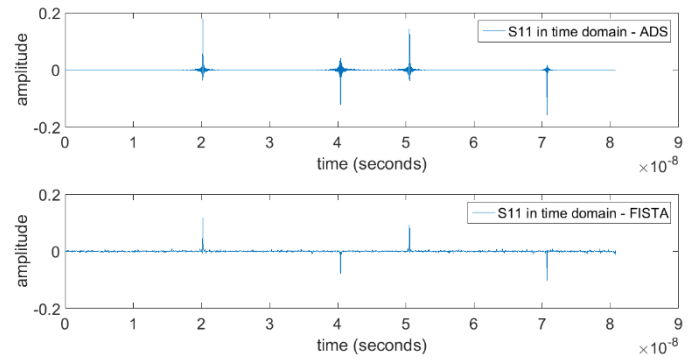


Fig. 5 - Comparison for  $S_{11}$  in time domain of the simulated line. Mean squared error:  $2.33 \cdot 10^{-08}$ .

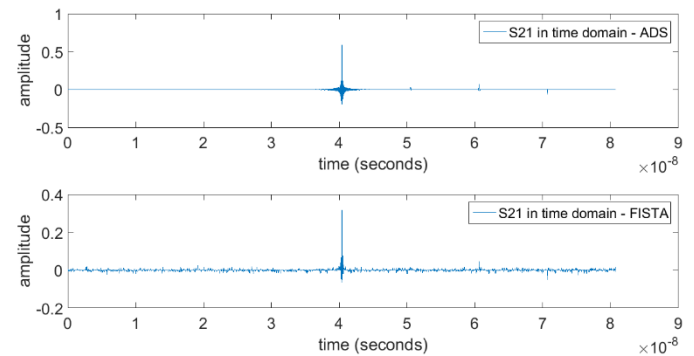


Fig. 6 - Comparison for  $S_{21}$  in time domain of the simulated line. Mean squared error:  $1.68 \cdot 10^{-04}$ .

Analyzing the results for the  $S_{11}$  parameter, it is possible to verify a positive reflection coefficient in about 20 ns. That reveals the transition from the first line to the second one, where there is an increasing of the impedance. This time value is related to the round trip of the wave, which gives the exact length for the constancy in the impedance along the line. After 40 ns, it is possible to see a negative reflection coefficient, revealing a decreasing of the impedance in that location. Following the line length there are two more changes like those. They are located and characterized as it is in the experimental transmission line topology.

The results for the  $S_{21}$  parameter in time domain give an insight for how the line under test behaves when transmitting data. From the  $S_{21}$  parameter it is possible to determine how long is the line. It is given by the location of the first impulse presented in the signal, while the magnitude of the first impulse will give the attenuation for any incident signal. Analyzing the results for  $S_{21}$  it is possible to verify that the line is over 40 ns long.

Both results are similar in location and shape comparing to the results in time domain obtained from the software ADS. The mean squared error for the  $S_{11}$  parameter obtained from the simulated analysis was  $2.33 \cdot 10^{-08}$ , whereas for the  $S_{21}$  parameter was  $1.68 \cdot 10^{-04}$ .

The results for the  $S_{11}$  and  $S_{21}$  parameter of the measured line are shown in Fig. 7 and Fig. 8 respectively.

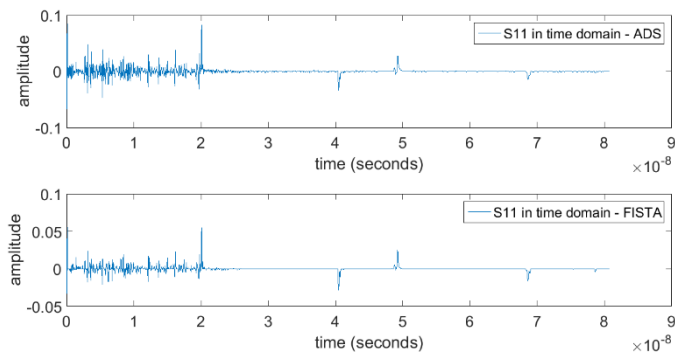


Fig. 7 - Comparison for  $S_{11}$  in time domain of the measured line. Mean squared error:  $1.20 \cdot 10^{-05}$ .

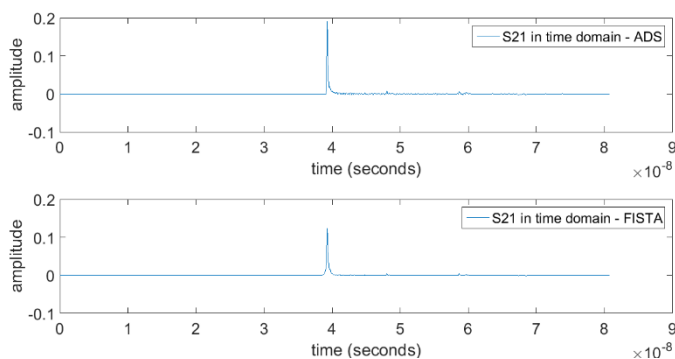


Fig. 8 - Comparison for  $S_{21}$  in time domain of the measured line. Mean squared error:  $6.20 \cdot 10^{-06}$ .

On the waveform of the  $S_{11}$  parameter in time domain, either for the simulated or the measured data analysis, it can be noted some noise presented until the first reflection occurs. The noise source is unknown, but it can be seen in both results, which enables to state that is not caused by the proposed method.

Both results show similarity in location and shape in comparison to the results in time domain obtained from the software ADS. The mean squared error for the  $S_{11}$  parameter obtained from the measured analysis was  $1.20 \cdot 10^{-05}$ , whereas for the  $S_{21}$  parameter was  $6.20 \cdot 10^{-06}$ .

## VII. CONCLUSIONS

This paper presented a sparse approach for the Inverse Chirp Z Transform. The method shows promising results in time domain analysis of S parameters, with good agreement in time location and wave shape of the signals compared to the results obtained from the software ADS.

## ACKNOWLEDGEMENTS

The authors acknowledge Petrobras and National Agency of Petroleum, Natural Gas and Biofuels for providing financial resources for this study.

## REFERENCES

- [1] Ching-Wen Hsue and Te-Wen Pan, "Reconstruction of nonuniform transmission lines from time-domain reflectometry," *IEEE Trans. Microw. Theory Tech.*, vol. 45, no. 1, pp. 32–38, 1997.
- [2] H. Vanhamme, "High Resolution Frequency-Domain Reflectometry," *IEEE Trans. Instrum. Meas.*, vol. 39, no. 2, pp. 369–375, 1990.
- [3] J. Dunsmore, N. Cheng, and Y. X. Zhang, "Characterizations of asymmetric fixtures with a two-gate approach," *2011 77th ARFTG Microw. Meas. Conf. Des. Meas. Microw. Syst. ARFTG 2011*, 2011.
- [4] T. V. Veijola and M. E. Valtonen, "Identification of cascaded microwave circuits with moderate reflections using reflection and transmission measurements," *IEEE Trans. Microw. Theory Tech.*, vol. 36, no. 2, pp. 418–423, 1988.
- [5] H. Van Hamme, "High-resolution frequency-domain reflectometry by estimation of modulated superimposed complex sinusoids," *IEEE Trans. Instrum. Meas.*, vol. 41, no. 6, pp. 762–767, 1992.
- [6] H. Vanhamme, "High resolution frequency-domain reflectometry," *IEEE Trans. Instrum. Meas.*, vol. 39, no. 2, pp. 369–375, Apr. 1990.
- [7] M. Zyari and Y. Rolain, "Identifying Multiple Reflections in Distributed-Lumped High-Frequency Structures," *IEEE Trans. Microw. Theory Tech.*, vol. 64, no. 4, pp. 1306–1312, Apr. 2016.
- [8] Agilent, "Time domain analysis using a network analyzer," *Appl. note 1287-12*, pp. 1–48, 2012.
- [9] R. Papazyan, P. Pettersson, H. Edin, R. Eriksson, and U. Gafvert, "Extraction of high frequency power cable characteristics from S-parameter measurements," *IEEE Trans. Dielectr. Electr. Insul.*, vol. 11, no. 3, pp. 261–270, Jun. 2004.
- [10] L. R. Rabiner, R. W. Schafer, and C. M. Rader, "The Chirp Z-Transform Algorithm," *IEEE Trans. Audio Electroacoust.*, vol. 17, no. 2, pp. 86–92, 1969.
- [11] D. A. Frickey, "Using the Inverse Chirp-Z Transform for Time-Domain Analysis of Simulated Radar Signals," *ICSPAT 94 signal Process. Appl. Technol.*, pp. 1–6, 1994.
- [12] R. M. Mersereau, "An Algorithm for Performing an Inverse Chirp Z-Transform," *IEEE Trans. Acoust.*, vol. 22, no. 5, pp. 387–388, 1974.
- [13] R. De Porrata-Dória i Yagüe, A. B. Ibars, and L. F. Martínez, "Analysis and Reduction of the Distortions Induced by Time-Domain Filtering Techniques in Network Analyzers," *IEEE Trans. Instrum. Meas.*, vol. 47, no. 4, pp. 930–934, 1998.
- [14] Agilent Technologies, "S-Parameter Design," *Application Note*

*AN154*, vol. 1. Agilent Technologies, pp. 1–44, 2006.

- [15] A. Beck and M. Teboulle, “Fast Gradient-Based Algorithms for strained Total Variation Image Denoising and Deblurring Problems,” *IEEE Trans. Image Process.*, vol. 18, no. 11, pp. 2419–2434, 2009.
- [16] Anritsu, “A Guide to Making RF Measurements for Signal Integrity Applications.” Anritsu, pp. 1–24, 2016.
- [17] Anritsu, “Cable Testing & Time Domain - VNA Roadshow 2016.” Anritsu, pp. 1–62, 2016.